A ONE-DIMENSIONAL MODEL OF WASTES COMBUSTION PROCESSES IN CEMENT ROTARY KILNS

B.-J.R. MUNGYEKO BISULANDU[1,2,*] and F. MARIAS[1]
[1]Laboratoire de Thermique, Energétique et Procédés (LaTEP), Ecole Nationale Supérieure de Génie et de Technologies Industrielles (ENSGTI), Université de Pau et des Pays de l'Adour (UPPA), Rue Jules Ferry, B.P. 7511, 64075 Pau Cedex, France.
[2]Optimisation énergétique des fours de cimenterie, Génie Mécanique-Energétique, Faculté Polytechnique, Université Kongo, B.P. 202 Mbanza-Ngungu, Kongo Central, RD Congo.
*Corresponding author: jean-robert.mungyeko-bisulandu@univ-pau.fr , +33 (0)540175193.

Abstract

Because of the depletion of fossil fuels and because of its increasing cost, waste has been used as alternative fuels in cement rotary kilns for several years. In order to fulfill the requirements of environmental protection and quality of the final product, it is necessary to understand and quantify the different processes occurring in the kiln. The aim of our work is to develop a mathematical model of the processes occurring in the kiln. This model will rely on the coupling between a CFD model and homemade software. More precisely, the CFD model, which will be fully three-dimensional will account for the homogeneous processes taking place in the freeboard of the bed of material being processed. This bed of material will be at the center of the second model which will represent it as a 1D plug flow reactor. In the present work, we focus on this 1D model. We first give insights on the main assumptions on which the model rely, and information on the reaction pathway leading to the production of cement. Indeed, it is considered that the bed is composed of a mixture of $CaCO_3$, $MgCO_3$, Al_2O_3, SiO_2, Fe_2O_3, MgO, CaO, C_2S, C_3A, C_4AF and C_3S undergoing thermochemical transformation. The bed under consideration is also composed of waste and biomass (tires, RDF, agricultural residues). During its transformation (pyrolysis, combustion of volatiles, combustion of the pyrolysis residue), this material contributes to thermal equilibrium of the reactor, by carrying the energy associated to its complete combustion. In this paper, the different equations that translate into mathematical formalism the processes of transport of the bed as well as mass and energy balance are also presented.

Keywords: Cement rotary kilns, Cement clinker, Wastes, Combustion processes, One-dimensional model.

1. INTRODUCTION

The use of renewable energy sources and waste recovery processes, particularly in the cement industry is rapidly increasing. Several reasons can be cited, including the scarcity of fossil energy sources, global warming, increasing waste, causing serious pollution problems in urban cities worldwide [1]. Our societies are highly dependent of fossil fuels. The depletion of these sources, might lead to a decrease in the productivity of our industries. The cement industry is not excluded from the list. The cement industry is considered as one of the most energy-intensive industry, with an energy consumption rate ranging from 30-40% of the final production cost, [2]. The largest share of energy consumption is in the workshop rotary kiln firing. Rotary kilns are mainly used in cement industries. Their role is to produce clinker for the manufacture of Portland cement. The clinker is obtained after cooking of the raw meal (fine material), consisting of a mixture of clay and limestone finely ground. Clinker production requires very high temperatures to initiate the reactions of sintering and phase changes necessary to form the complex compounds of clinker minerals, which are C_2S, C_3A, C_4AF and

C_3S, that give cement its unique properties [3]. Thus, for constantly respond to energy needs of rotary kilns, cement producers have increased the use of alternative fuels in partial replacement of fossil fuels [4], [5]. The use of renewable fuels, especially tire, RDF and biomass, requires knowledge of certain parameters, the most important of which are the elementary mass composition and the lower calorific value [5]. However, the choice is currently mainly based on price and availability. Several studies have been conducted with respect to the use of waste and biomass in rotary kilns. Kaddatz et al [6] studied the use of alternative fuels (used industrial lubricants, used tires) in cement kilns and their impacts in the process. It follows from these studies that the intrinsic properties of sintering in a rotary kiln favors combustion of a large number of fuels which are often banned as fuel in other processes. These studies have also noted that the used industrial lubricants and used tires were more adapted to replace coal, because of their energy content and because of the lowest overall emissions of carbon dioxide they generate. Di Blasi [7] observed that the biomass and waste are widely recognized to be a significant potential for energy production. Alternative fuels are economically very interesting, insofar as they provide the equivalent power (PCI) than fossil fuels and this at a lower cost. However, their use in the cement manufacturing process can have as a major risk, degradation of cement quality. Aranda and al [8], in their study, have approximately given a ratio of 20% for biomass which may be substituted in cement rotary kiln, while maintaining a stable combustion process and the quality of the clinker. Hence there is a need for a better understanding of the thermochemical phenomena taking place in the kiln. This is the reason why we propose to develop a model of thermochemical processing of meal (cement) and waste in a cement rotary kiln. This model must take into account the heat transfer in the kiln shell, physicochemical phenomena in the freeboard as well as the physicochemical changes occurring in the bed (bed Model). The final model will be a coupling between CFD Fluent model, 1D model of the bed, and the kiln shell. The objective of this article is the description of the 1D model of bed, identifying the main assumptions of the model, describing the system of study, and finally proposing equations of the 1D model. Note that the results of the bed 1D model are not yet available at this time.

1.1. Cement manufacturing process

There are five main steps in the cement manufacturing process:

- The extraction of raw materials in the career and its homogenization;
- The preparation of raw materials in order to constitute the raw meal (or paste for wet method);
- The cooking of meal leading to the creation of clinker;
- The grinding of clinker and additions to make cement, and;
- The storage and dispatch of cement.

Cement manufacturing can take place regardless of the production of clinker. We know that the main raw materials used in the manufacture of cement are limestone ($CaCO_3$, $MgCO_3$…) and clay ($Al_2O_3.nSiO_2.mFe_2O_3.wH_2O$) and/or marl, material in which the two components are already naturally mixtures [9]. After extraction to the career, these components are crushed, then ground and dried by combustion gases exhausting the rotary kiln. Depending on the type of cement to produce, the following products may be added: pyrite ash, fly ash from coal power plants, clay sand and ash from electrostatic filters [10]. The mixture is obtained (raw meal) after grinding of 80 % of limestone and 20 % of clay. It is then sent to homogenizers silos to obtain the homogenized meal, and finally fed to the rotary kiln for firing and obtaining clinker. 97% of clinkers are ground with 3% of gypsum ($CaSO_4.2$ (H_2O)), to finally give cement. C_2S, C_3A, C_4AF and C_3S are the four mineralogical components of the clinker. They are accompanied by minor elements such as free lime (free CaO), periclase (MgO), alkalis, heavy metals… that affect the quality of clinker produced [11].

1.2. Aspects associated to the modeling of rotary kilns

The modeling of cement production in rotary kiln with use of alternative fuels can be done in various aspects, including the aspects related to transport of the load in the rotary kiln, to the cement chemistry, to the chemistry and physic of the combustion of waste, to heat transfer in the bed, in the gas and in the walls (envelope) of the kiln, etc... -To take into account the whole set of these phenomena, we have chosen to build our model as an assembly of three submodels:

- Modeling the bed of material (1D): mixture "Meal-Waste-Gas" (aim of this article),
- Modeling the freeboard (gas phase) (3D), including radiation and homogeneous reaction phenomena using CFD;
- Modeling the kiln shell (1D): refractory + metal sheet.

The figure 1 gives a representation of the assembly of these submodels.

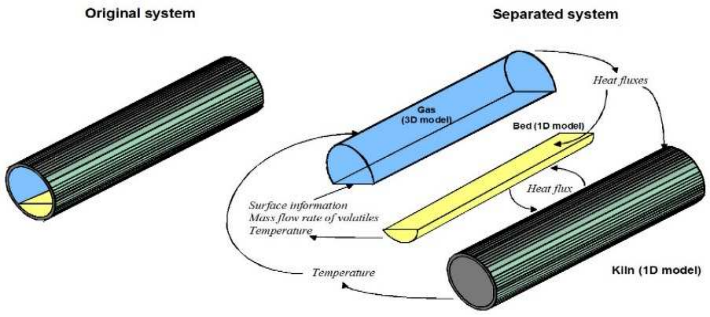

Figure 1: Scheme of different models of rotary kiln

The key issues governing the performance of cement rotary kilns when waste is used, are shown schematically in figure 2 below. At the inlet end, the waste is introduced into the furnace together with the flour from precalciner. The gases produced by the burner in the kiln circulating in counter current flow, exchanges energy with the solid bed and the kiln walls. The kiln walls exchange energy with the solid bed and the external environment. From the other end, the secondary air is introduced for the combustion of fossil fuel, and, at the same time the clinker leaves the kiln at approximately 1723.15 K.

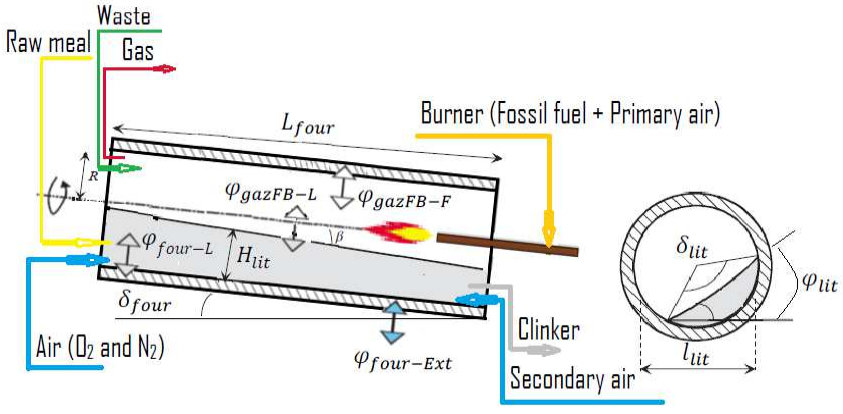

Figure 2: Representation of the processes occurring in the rotary kiln

Boateng et al [12] in their studies on the thermal model of heat transfer in the bed, affirmed that the possibility to simulate the freeboard transport phenomena is greater than the capacity to determine precisely the conditions in the bed. Marias [13], in its work, assumed that the bed receives the specific heat flow of the gas phase and the specific heat flow of the kiln walls.

2. ASSUMPTIONS OF THE MODEL

2.1. Assumptions

In the present work, we consider the bed as being constituted of raw meal, waste (and/or biomass) and gas. At the inlet end, all proportions (mass fractions of species) are assumed to be known. It is assumed that the gas at the inlet is air, with N_2 and O_2, respective contents of 79 % and 21 %. Meal having already undergone some transformations since its admission to the cyclone preheaters, passing through the calciner, it enters the rotary kiln with a temperature ranging from 800 - 900 °C. Given this value of temperature, pyrolysis of alternative fuel occurs as it is fed to the kiln. Because of the level of temperature encountered in the kiln, it is thereafter assumed that the whole set of pyrolysis reactions can be lumped into a single step reaction. Some details regarding the composition of the products of this reaction will be given latter in the text. The overall production of CO_2 is therefore the sum of CO_2 fractions produced by decarbonation reactions of meal,

$$CaCO_3 + 178\ MJ/mol \rightarrow CaO + CO_2 \quad (R1)$$

$$MgCO_3 + 109\ MJ/mol \rightarrow MgO + CO_2 \quad (R2)$$

and by the pyrolysis of waste, and subsequent combustion of waste. Considering that in the calciner, decomposition (decarbonation) of $CaCO_3$ takes place with yields ranging from 90 to 95%, the chemical reaction above continues into the rotary kiln [14]. In our case, we estimate the remaining amount of $CaCO_3$ to be 10 % of the input content. The total decomposition of $MgCO_3$ occurs in the calciner. The activation energy required by decarbonation reaction comes from the heat of combustion of fossil fuels (coal, fuel oil) burned in the burner of rotary kiln and from the combustion of the products of pyrolysis. Regarding the activation energy of waste pyrolysis reaction, it comes from the sensible heat of the meal. The main assumptions of our model are the following:

- The bed of material under thermochemical transformation is considered as 1D plug flow model (perfect mixing in every slice of the bed);
- Each tranche (slice) is composed of:
  - **Solid Meal**, composed of the following species: $CaCO_3$, $MgCO_3$, Al_2O_3, SiO_2, Fe_2O_3, MgO, CaO, C_2S, C_3A, C_4AF and C_3S;
  - **Liquid Meal**, composed of the following species: C_3A and C_4AF;
  - **Waste**, composed of Organic Matter (C, H, O, N, S and Cl), of Char (C), of Ashes, and of Moisture (H_2O liquid), and;
  - **Gas**, composed of air (N_2 and O_2), of products of pyrolysis reaction (CH_4, H_2, H_2O, CO, CO_2, H_2S, HCN, HCl, C_6H_6, $C_{10}H_8$, C_6H_6O, and C_7H_8), and their combustion (CO_2 and H_2O), and of NO.
- The bed is in plug flow, its properties are given in terms of its axial position (z);
- In every slice of the bed, there is a thermal equilibrium between all the materials held in the slice. Hence, all these materials share the same temperature and there is no heat transfer between them. It has to be noticed however that neither the kiln nor the freeboard share the same temperature;
- Bed transport (and all its components) is described as a translation from the input to the output of the bed. The velocity at which this translation occurs depends on the operating parameters of the bed;
- At every axial position, the bed receives heat fluxes from the kiln and the freeboard gas;
- The formation of melt phase depends on the local temperature and the of the presence of two oxides (Al_2O_3 and Fe_2O_3) in the bed;
- Particles of waste are assume to be spherical as they are fed to the kiln. During pyrolysis process it preserves its spherical shape with a constant diameter, although its porosity increases;
- The distribution of volatiles remains constant when the pyrolysis reaction proceeds

- Ashes are considered inert. Its thermal capacity is estimated at 1000 $kJ.kg^{-1}.K^{-1}$.

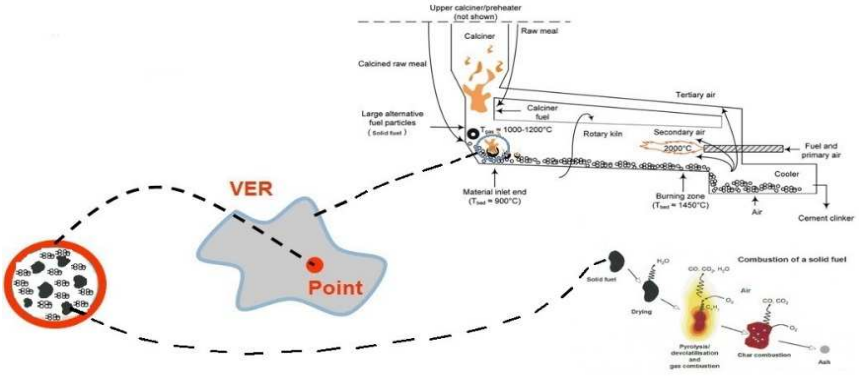

Figure 3: Waste recovery in rotary kiln

2.2. Reactions

2.2.1. Solid Meal

The chemical reactions occurring during clinker formation are given in the table 1 below, where y_k^{Sol} represent the mass fraction of species K in the solid meal.

Reactions	**Reactions rates** [s^{-1}]	**Kinetic constants** [s^{-1}]	**Ref.**
$CaCO_3 \xrightarrow{k_{f1}} CaO + CO_2$	$r_{f1} = k_{f1}.y_{CaCO_3}^{Sol}$	$k_{f1} = 4{,}55 \times 10^{31} exp\left(\frac{-7{,}81 \times 10^5}{\mathcal{R}T_{lit}}\right)$	[14]
$MgCO_3 \xrightarrow{k_{f2}} MgO + CO_2$	$r_{f2} = k_{f2}.y_{MgCo_3}^{Sol}$	$k_{f2} = 9{,}9 \times 10^6 exp\left(\frac{-1{,}5 \times 10^5}{\mathcal{R}T_{lit}}\right)$	[15]
$2CaO + SiO_2 \xrightarrow{k_{f3}} C_2S$	$r_{f3} = k_{f3}.y_{SiO_2}^{Sol}.(y_{CaO}^{Sol})^2$	$k_{f3} = 4{,}11 \times 10^5 exp\left(\frac{-1{,}93 \times 10^5}{\mathcal{R}T_{lit}}\right)$	[14]
$C_2S + CaO \xrightarrow{k_{f4}} C_3S$	$r_{f4} = k_{f4}.y_{C_2S}^{Sol}.y_{CaO}^{Sol}$	$k_{f4} = 1{,}33 \times 10^5 exp\left(\frac{-2{,}56 \times 10^5}{\mathcal{R}T_{lit}}\right)$	[14]
$3CaO + Al_2O_3 \xrightarrow{k_{f5}} C_3A$	$r_{f5} = k_{f5}.(y_{CaO}^{Sol})^3.y_{Al_2O_3}^{Sol}$	$k_{f5} = 8{,}33 \times 10^6 \ exp\left(\frac{-1{,}94 \times 10^5}{\mathcal{R}T_{lit}}\right)$	[14]
$4CaO + Al_2O_3 + Fe_2O_3 \xrightarrow{k_{f6}} C_4AF$	$r_{f6} = k_{f6}.(y_{CaO}^{Sol})^4.y_{Al_2O_3}^{Sol}.y_{Fe_2O_3}^{Sol}$	$k_{f6} = 8{,}33 \times 10^8 exp\left(\frac{-1{,}85 \times 10^5}{\mathcal{R}T_{lit}}\right)$	[14]

Table 1: Reactions and reactions rates used in the model for solid meal (chemical transformation)

2.2.2. Liquid Meal

The chemical reactions occurring during physical transformation of meal are given in the table 2 below, where $\overline{[k]}$ represent the mass concentration of the species of the solid meal that transform into liquid meal.

Reactions	**Reactions rates** [$kg.m^{-3}.s^{-1}$]	**Kinetic constants** [s^{-1}]
$C_3A \xrightarrow{k_{fl1}} (C_3A)_{Liq}$	$r_{fl1} = k_{fl1}\overline{[C_3A]}$	$k_{fl1} = 3{,}78 \times 10^5 \ exp\left(\frac{-234{,}12 \times 10^3}{\mathcal{R}T_{lit}}\right)$
$C_4AF \xrightarrow{k_{fl2}} (C_4AF)_{Liq}$	$r_{fl2} = k_{fl2}\overline{[C_4AF]}$	$k_{fl2} = 2{,}01 \times 10^8 \ exp\left(\frac{-203{,}42 \times 10^3}{\mathcal{R}T_{lit}}\right)$

Table 2: Reactions and reactions rates used in the model for Liquid meal (physical transformation)

2.2.3. Pyrolysis

The reaction of waste pyrolysis is presented as follows:

$$C_{\alpha1}H_{\beta1}O_{\gamma1}N_{\delta1}S_{\varepsilon1}Cl_{\omega1}.cdr_1 \rightarrow \nu_C C.cdr_1 + \nu_{H_2}H_2 + \nu_{CH_4}CH_4 + \nu_{CO}CO + \nu_{H_2O}H_2O + \nu_{CO_2}CO_2 + \nu_{H_2S}H_2S + \nu_{HCl}HCl + \nu_{HCN}HCN + \nu_{C_6H_6}C_6H_6 + \nu_{C_{10}H_8}C_{10}H_8 + \nu_{C_6H_6O}C_6H_6O + \nu_{C_7H_8}C_7H_8 \quad (R3)$$

Where the coefficients ν_i stand for the mass stoichiometric coefficients of the reaction (kg/kg of waste). These coefficients are calculated on the basis of material balances, and given experimental information on the pyrolysis of the considered material. It is also expected that the solid residue of pyrolysis (char) is composed of pure carbon.

2.2.4. Combustion and gasification of solid pyrolysis residue

The 1D model takes into account the heterogeneous reactions of combustion and gasification of char given in the table 3 below. The Shell Progressive (SP) model is used in this work.

Reaction	**Tire** [16]		**RDF** [7]		**Biomass**[7]	
	A [s^{-1}]	**E** [$J.mol^{-1}$]	**A** [s^{-1}]	**E** [$J.mol^{-1}$]	**A** [s^{-1}]	**E** [$J.mol^{-1}$]
$2C + 1{,}5O_2 \xrightarrow{kc18} CO + CO_2$	$2.3T_{lit}$	$11100\mathcal{R}$	$5.67x10^9$	160	$5.67x10^9$	160
$C + CO_2 \xrightarrow{kg1} 2CO$	$589T_{lit}$	$26800\ \mathcal{R}$	$7.93x10^4$	218	$7.93x10^4$	218
$C + H_2O \xrightarrow{kg2} CO + H_2$	$589T_{lit}$	$26800\ \mathcal{R}$	$7.92x10^4$	218	$7.92x10^4$	218

Table 3: Heterogeneous reaction and Kinetics constants of char

The Shell Progressive model states that in the heterogeneous reaction, the ash layer remains on the particle; consequently the particle diameter D_{dec} remains constant, while the diameter of the core of the char d_c is reduced by reaction progress (figure 4).

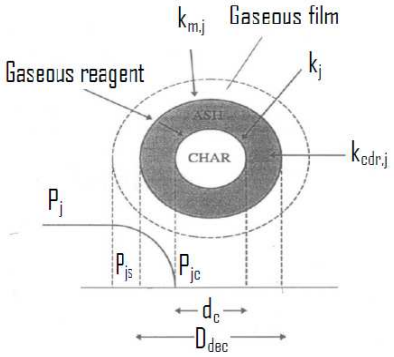

Figure 4: Shell Progressive model

2.2.5. Mass loss of solid and evolution of the bed height

The mass loss of the solid bed is due primarily to the release of CO_2 during decomposition reactions (decarbonisation) of $CaCO_3$ and $MgCO_3$ contained in the meal, and secondly to the released of gaseous species by pyrolysis reactions. These gases are sent into the freeboard. The evolution of the bed height is heavily dependent on mass loss in the bed of solids and geometric parameters of bed and kiln. In this article, this evolution is accounted for by changes in geometrical parameters such as the angle of intercept angle of bed and repose angle of bed (kiln slope).

2.2.6. Transport of the charge

The transport in this type of kiln plays a key role in combustion or calcination of the load (Meal and/or waste). It is favoured by the inclination and the rotation speed of kiln. These latter allow to modulate the residence time of charge (meal and waste) in the kiln. From six bed motions (ie slipping, slumping, rolling, cascading, cataracting and centrifuging) in a rotary kiln (see figure 5), only the rolling is desirable because it occurs at relatively low speeds, and promotes a good mix of particles in the bed, with a rapid renewal of the bed surface exposed on the freeboard.

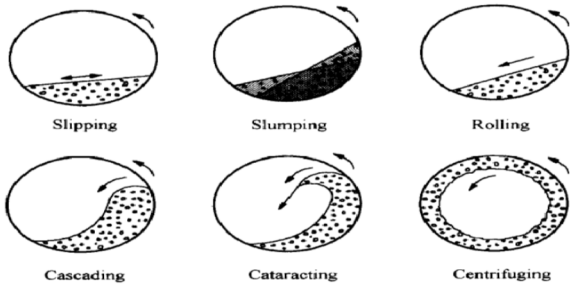

Figure 5: Motions of the material bed [17]

2.2.7. **Reactions in homogeneous phase** (combustion of the volatiles)

Table 4 below gives the different homogeneous reactions that are taken into account in this model. $[b]$ are molar concentrations of "b" species in gas phase (kmol.m^{-3}).

Reactions	**Reaction rate** $[kmol.m^{-3}.s^{-1}]$	**Kinetic constants** $[s^{-1}]$	**Ref.**
$CH_4 + H_2O \xrightarrow{kc1} CO + 3H_2$	$R_{c1} = k_{c1}[CH_4].[H_2O]$	$k_{c1} = 3{,}101 \times 10^3 exp\left(\frac{-1{,}247 \times 10^5}{\mathcal{R}T_{lit}}\right)$	[18]
$CO + H_2O \xrightarrow{kc2} CO_2 + H_2$	$R_{c2} = k_{c2}[CO].[H_2O]$	$k_{c2} = 2{,}778 \times 10^2 exp\left(\frac{-1{,}256 \times 10^4}{\mathcal{R}T_{lit}}\right)$	[18]
$CO_2 + H_2 \xrightarrow{kc3} CO + H_2O$	$R_{c3} = k_{c3}[CO_2].[H_2]$	$k_{c3} = 1{,}263 \times 10^4 exp\left(\frac{-4{,}729 \times 10^4}{\mathcal{R}T_{lit}}\right)$	[18]
$H_2O + CO \xrightarrow{kc4} CO_2 + H_2$	$R_{c4} = k_{c4}[H_2O].[CO]$	$k_{c4} = 2{,}780\ exp\left(\frac{-1{,}255 \times 10^7}{\mathcal{R}T_{lit}}\right)$	[19]
$CO + 0{,}5O_2 \xrightarrow{kc5} CO_2$	$R_{c5} = k_{c5}[CO].[H_2]^{0,25}.[H_2O]$	$k_{c5} = 10^{17{,}6} exp\left(\frac{-1{,}660 \times 10^5}{\mathcal{R}T_{lit}}\right)$	[19]
$H_2 + 0{,}5O_2 \xrightarrow{kc6} H_2O$	$R_{c6} = k_{c6}[O_2].[H_2]$	$k_{c6} = 1{,}08 \times 10^{10} exp\left(\frac{-1{,}255 \times 10^5}{\mathcal{R}T_{lit}}\right)$	[18]
$CO + 0{,}5O_2 \xrightarrow{kc7} CO_2$	$R_{c7} = k_{c7}[CO].[O_2]^{0,25}.[H_2O]^{0,5}$	$k_{c7} = 3{,}165 \times 10^{12} exp\left(\frac{-1{,}8 \times 10^5}{\mathcal{R}T_{lit}}\right)$	[19]
$CH_4 + 2O_2 \xrightarrow{kc8} CO_2 + 2H_2O$	$R_{c8} = k_{c8}[CH_4]^{0,3}.[O_2]^{1,3}$	$k_{c8} = 1{,}3 \times 10^5 exp\left(\frac{-2{,}025 \times 10^5}{\mathcal{R}T_{lit}}\right)$	[18]
$CH_4 + 0{,}5O_2 \xrightarrow{kc9} CO + 2H_2$	$R_{c9} = k_{c9}[CH_4]^{0,7}.[O_2]^{0,8}$	$k_{c9} = 4{,}996 \times 10^{13} exp\left(\frac{-2{,}026 \times 10^5}{\mathcal{R}T_{lit}}\right)$	[18]
$C_6H_6 + \frac{15}{2}O_2 \xrightarrow{kc10} 6CO_2 + 4H_2O$	$R_{c10} = k_{c10}[C_6H_6]^{-0,1}.[O_2]^{1,25}$	$k_{c10} = 1{,}783 \times 10^1 exp\left(\frac{-1{,}255 \times 10^5}{\mathcal{R}T_{lit}}\right)$	[18]
$C_6H_6 + 3O_2 \xrightarrow{kc11} 6CO + 3H_2$	$R_{c11} = k_{c11}[C_6H_6].[O_2]$	$k_{c11} = 1{,}58 \times 10^{15} exp\left(\frac{-2{,}026 \times 10^5}{\mathcal{R}T_{lit}}\right)$	[18]
$C_6H_6 + 5H_2O \xrightarrow{kc12} 5CO + 6H_2 + CH_4$	$R_{c12} = k_{c12}[C_6H_6]$	$k_{c12} = 4{,}4 \times 10^8 exp\left(\frac{-2{,}2 \times 10^5}{\mathcal{R}T_{lit}}\right)$	[18]
$C_7H_8 + H_2 \xrightarrow{kc13} C_6H_6 + CH_4$	$R_{c13} = k_{c13}[C_7H_8].[H_2]^{0,5}$	$k_{c13} = 1{,}04 \times 10^{12} exp\left(\frac{-2{,}47 \times 10^5}{\mathcal{R}T_{lit}}\right)$	[18]
$C_7H_8 + 9O_2 \xrightarrow{kc14} 7CO_2 + 4H_2O$	$R_{c14} = k_{c14}[C_7H_8]^{-0,1}.[O_2]^{1,25}$	$k_{c14} = 1{,}426 \times 10^1 exp\left(\frac{-1{,}255 \times 10^5}{\mathcal{R}T_{lit}}\right)$	[18]
$C_{10}H_8 + 4H_2O \xrightarrow{kc15} C_6H_6 + 4CO + 5H_2$	$R_{c15} = k_{c15}[C_{10}H_8].[H_2]^{0,4}$	$k_{c15} = 1{,}74 \times 10^{12} exp\left(\frac{-3{,}24 \times 10^5}{\mathcal{R}T_{lit}}\right)$	[18]
$C_6H_6O + \frac{11}{2}O_2 \xrightarrow{k16} 6CO_2 + 3H_2$	$R_{c16} = k_{c16}[C_6H_6O]^{-0,1}.[O_2]^{1,85}$	$k_{c16} = 2{,}4 \times 10^{11} exp\left(\frac{-1{,}25 \times 10^5}{\mathcal{R}T_{lit}}\right)$	[20]
$C_6H_6O + 4H_2O \xrightarrow{kc17} CO + 0{,}4C_{10}H_8 + 0{,}15C_6H_6 + 0{,}1CH_4 + 0{,}75H_2$	$R_{c17} = k_{c17}[C_6H_6O]$	$k_{c17} = 10^7 exp\left(\frac{-1{,}0 \times 10^5}{\mathcal{R}T_{lit}}\right)$	[20]

Table 4: Reactions and Kinetics in gas phase

2.3. Different variables in the 1D model

The set of variables taken into account in the model is the following:

Variables	Notification	Amount	Unit
y_k^{Sol}	Mass fraction of species K in the Solid Meal	NESFASOL	-
y_k^{Liq}	Mass fraction of species K in the Liquid Meal	NESFALIQ	-
y_{fa}^{Sol}	Mass fraction of Solid Meal in the Meal	1	-
y_{fa}^{Liq}	Mass fraction of Liquid Meal in the Meal	1	-
y_{fa}^{lit}	Mass fraction of Meal in the Bed	1	-
y_d^{MO}	Mass fraction of species D in the Organic Matter	NESMO	-
y_q^{dec}	Mass fraction of species Q in the waste	NESDEC	-
y_{dec}^{lit}	Mass fraction of Waste in the Bed	1	-
D_{dec}	Diameter of Waste particle	1	m
N_{dec}	Number of waste particles	1	m^{-3}
y_b^{gaz}	Mass fraction of species B in the Gas	NESGAZ	-
y_{gaz}^{lit}	Mass fraction of Gas in the Bed	1	-
ρ_{lit}	Bed density	1	$kg.m^{-3}$
T_{lit}	Bed temperature	1	K
h_{lit}	Enthalpy of the Bed	1	$J.mol^{-1}$
u_{lit}	Bed Velocity	1	$m.s^{-1}$
H_{lit}	Bed height	1	m
A_{lit}	Transversal surface of the Bed	1	m^2
l_{lit}	Width of Bed (or mid cord)	1	m
δ_{lit}	Intercept angle of Bed	1	degree
φ_{lit}	Repose angle of Bed (or Kiln slope)	1	degree
β	Angle between plane surface of Bed material and kiln axis	1	degree

Table 5: 1D model variables

With NESFASOL=11; NESFALIQ=2; NESMO=6; NESDEC=4, and; NESGAZ=15.

3. SYSTEM UNDER STUDY

3.1. Description of waste

For our study, we consider three types of waste, namely Tires, RDF and Biomass.

3.1.1. Waste Tires

Waste resulting from tires have a high calorific value (it is the same order of magnitude as the one of coal), and the same content of carbon (char) [1]. Considering the increasing number of trucks and cars in circulation, used tires are increasingly abundant. These tires can be recycled or otherwise disposed in order to solve the problem of environmental pollution, and reduce emissions of greenhouse gases when waste is burned separately (waste burnt in incinerators without any goal energy recovery or material). The UE alone generates annually about 3.3 million tons of used tires. An important part (1.15 million tons) are already used in the cement kiln industry as alternative fuels [21]. Table 6 below, provides information on the proximate and ultimate analysis of such materials.

3.1.2. Refuse Derived Fuel (RDF)

The RDF is a mixture of several wastes, including household waste, municipal solid waste (MSW), plastics, and biodegradable materials. These latter are found in large quantities in the RDF. It is indeed used in many industrial processes: pyrolysis, gasification, combustion and others. RDF provides solutions for the disposal of fractions of non-recyclable waste, because it can be used as a direct substitute for fossil fuels in gasification [22]. The high content in ash and volatile matter in the RDF can lead to low heat production, thereby creating a high ash sintering, and an increase tar and CO_2 emissions. The RDF in question here, is formed from a

mixture of 50 % of industrial waste, and 50 % of municipal solid waste (MSW), cf. Table 6 below.

3.1.3. Agricultural residues (Biomass)

Biomass is one of the most used wastes as alternative fuels in industrial processes and in the cement industry due to their availability and very low price. It consists of different residues of agriculture, such as bagasse, peanut shells, almonds shells, straw, rice husks and coffee husks as well as residues from forest-related activities such as wood chips, sawdust and bark. The use of biomass to provide partial substitution of fossil fuels, has an additional importance as concerns global warming since biomass combustion has the potential to be CO_2 neutral. This is particularly the case with regard to agricultural residues or energy plants, which are periodically planted and harvested [23]. The agricultural residues are characterized by higher contents of volatile matter, compared with others waste (see table 6 below), and coals.

Elements	**Tire** [24]	**RDF** [22]	**Biomass** [8]
Proximate analysis (Raw material)	**% mass**	**% mass**	**% mass**
Organic Matter	94.6	62.4	95.77
Char	0	0	0
Ashes	4.78	23.2	4.2
Moisture	0.62	14.4	7.6
Ultimate analysis (Dry ash free)	**% mass**	**% mass**	**% mass**
C	83.87	47	48.73
H	7.09	6.3	5.9
O	7.421	44.6	44.49
N	0.24	1.7	0.6
S	1.23	0.1	0.08
Cl	0.149	0.3	0.2
Lower calorific Value (Raw material), in MJ/kg	37.8	29.86	17.97

Table 6: Elemental and proximate analysis, and calorific value of different wastes.

3.2. Pyrolysis description of waste considered

Pyrolysis of waste occurs after the drying process, which releases the free water contained in waste. Drying phenomenon is described using a diffusion model, which stated that the rate of vaporisation of water depends on difference between the concentration of water at saturation and in the bed.

$$R_{H_2O\_liq}^{hét} = \nu_p \, k_{m,H2O} \left(\frac{p_{H2O}^{sat} M_{H2O}}{RT_{lit}} - \rho_{H_2O}^{gaz} \right) \quad (1)$$

Pyrolysis of waste considered takes place in a single reaction (primary pyrolysis) to give char (carbon-based powder), the non-condensable gases such as CH_4, H_2, H_2O, CO, CO_2, H_2S, HCN and HCl, and tar constituted of C_6H_6, $C_{10}H_8$, C_6H_6O, and C_7H_8 (condensable gases). The pyrolysis kinetic of waste considered, follows the Arrhenius law, and is given in the table 7:

Pyrolysis reaction	**Reaction rate** $[kg.m^{-3}.s^{-1}]$	**Kinetic constant** $[s^{-1}]$
$WET\ WASTE \overset{k_v}{\rightarrow} DRY\ WASTE + (H_2O)_{vapeur}$	-	-
$DRY\ WASTE \overset{k_p}{\rightarrow} \alpha_{Ch} CHAR + \alpha_G GAS + \alpha_T TAR$	$r_p = k_p \rho_{waste}$	$k_p = A_p exp\left(\frac{-E_p}{.RT_{lit}}\right)$

Table 7: Pyrolysis reaction and Arrhenius law

The values of stoichiometric coefficients, kinetic constants and, gas and tar composition from pyrolysis reaction are given in the table 8 below.

Elements	Waste		
	Tire	RDF	Biomass
α_{Ch}	40	40	40
α_G	45.63	55.07	54.23
α_T	14.37	4.93	5.77
A_p [s^{-1}]	$5.02x10^{10}$ [25]	$1.27x10^{6}$ [26]	$1.516x10^{3}$ [7]
E_p[$kJ.mol^{-1}$]	148.06 [25]	22.9 [26]	105 [7]
Δh[$kJ.kg^{-1}$]	-	-	-420 [7]
H_2	16.42	0.29	0.3
CH_4	16.19	1.79	1.85
CO	1.548	5.64	5.8
H_2O	8.154	36.7	37.7
CO_2	1.351	6.85	7.05
H_2S	1.262	0.09	0.07
HCl	0.14	0.25	0.17
HCN	0.563	3.49	1.27
C_6H_6	4.70	1.50	1.75
$C_{10}H_8$	2.864	0.91	1.07
C_6H_6O	2.826	1.24	1.46
C_7H_8	3.985	1.27	1.49

Table 8: Stoichiometric coefficients and kinetics constants, composition of gas and tar (in %)

3.3. Description of the kiln studied

The kiln studied is a rotary kiln dry process with preheater, equipped with a precalciner and cooler balloon. The kiln has a length of 58 m, an inner diameter of 4 m and an outer one of 4.2 m. Its inclination is 3.5° while its rotation speed is 3.3 rpm. 40 to 62 t/h of raw material are fed to the kiln. The inlet and outlet temperatures are respectively 1173.15 K and 1723.15 K maximum.

4. MODEL FORMULATION

4.1. The solid bed

4.1.1. Number of particles

The concentration of waste (and/or biomass) particles inside the kiln being is considered constant, the equation (3) below is established:

$$\frac{dN_{dec}(z)}{dz} = 0 \quad (3)$$

At the entrance of the rotary kiln, the number of particles is largely function of volumetric flow rate of waste. It is given by the relation (4):

$$N_{dec}(z=0) = \frac{6q_v}{\pi\rho_{lit,0}D_{dec,0}^3 u_{lit}} y_{dec,0}^{lit} \quad (4)$$

4.1.2. Solid bed

4.1.2.1. Composition (mass fraction)

The mass balance in the length elemental of rotary kiln is given by a figure 6 below:

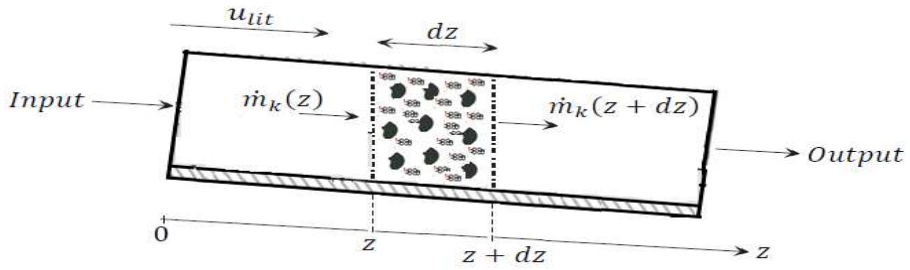

Figure 6: Mass balance through the kiln

The mass balances are given by the following relationships for each bed species under consideration, where the first member represents the variation of mass flow of the bed species (meal, waste, gas) and the right hand side represents the species formation rate onto a given bed cross sectional area of the bed. The bed being composed of meal, and waste, and gas, the conservation equations of bed species are also established, respectively given by equations (9), (11), and (14) below.

A. Meal

A1. Solid Meal

The mass conservation equation of the species k of the solid meal is modeled as follows:

$$\frac{d}{dz}\left(\rho_{lit}A_{lit}u_{lit}y_{fa}^{lit}y_{fa}^{Sol}y_{k}^{Sol}\right) = A_{lit}\left(R_k^{Ch,Sol} - R_k^{Ph}\right) \quad (5)$$

Where subscript k represent solid species of the raw meal being processed and stand for $CaCO_3$, $MgCO_3$, Al_2O_3, SiO_2, Fe_2O_3, MgO, CaO, C_2S, C_3A, C_4AF, and C_3S. The last four species are formed after clinkering reactions. They are in fact combinations of the four oxides (CaO, Al_2O_3, SiO_2, and Fe_2O_3). Mass fractions of four mineralogical compounds of clinker are considered to be zero at the entrance, but increases from the inlet to the outlet. The reaction terms $R_k^{Ch,Sol}$ and R_k^{Ph} are calculated based on the data in tables 1 and 2 respectively.

A2. Liquid Meal

Regarding the liquid meal, we have the equation (6) below, where k represents the species C_3A_liq, and C_4AF_liq which constitute the liquid meal.

$$\frac{d}{dz}\left(\rho_{lit}A_{lit}u_{lit}y_{fa}^{lit}y_{fa}^{Liq}y_{k}^{Liq}\right) = A_{lit}\left(R_k^{Ch,Liq} + R_k^{Ph}\right) \quad (6)$$

The meal being composed of two phases, solid and liquid, the mass conservation equations for each phase are modeled by equations (7) and (8) below:

- ***For Solid phase***

$$\frac{d}{dz}\left(\rho_{lit}A_{lit}u_{lit}y_{fa}^{lit}y_{fa}^{Sol}\right) = A_{lit}\left\{\sum_k R_k^{Ch,Sol} - \sum_k R_k^{Ph}\right\} \quad (7)$$

- ***For Liquid phase***

$$\frac{d}{dz}\left(\rho_{lit}A_{lit}u_{lit}y_{fa}^{lit}y_{fa}^{Liq}\right) = A_{lit}\left\{\sum_k R_k^{Ch,Liq} + \sum_k R_k^{Ph}\right\} \quad (8)$$

The last two equations (7) and (8) represent the sum of the conservation equation of k species of solid meal and liquid meal. The mass conservation equation meal in the bed is modeled by the equation (9), which is the sum of the mass conservation equations of two phases constituent of meal.

$$\frac{d}{dz}\left(\rho_{lit}A_{lit}u_{lit}y_{fa}^{lit}\right) = A_{lit}\left\{\sum_k R_k^{Ch,Sol} + \sum_k R_k^{Ch,Liq}\right\} \quad (9)$$

Liquid phase reactions are in fact due to the partial fusion of two species, the C_3A and C_4AF (physical transformation). Since a physical transformation (deformation, phase change, dissolution) does not change the nature or characteristic properties of matter (atoms and molecules do not change), we consider that $R_k^{Ch,Liq}$ are identical to $R_k^{Ch,Sol}$. Some authors attribute the formation of the liquid phase to the presence of aluminum and iron, and say that the liquid phase is the basis for the formation of additional coating (adhesive), which has the advantage of protecting refractory materials against wear having regard to the thermal constraints that they are facing [29].

B. Waste

The mass conservation equation of q waste species is modeled by the equation (10) below:

$$\frac{d}{dz}\left(\rho_{lit}A_{lit}u_{lit}y_q^{dec}y_{dec}^{lit}\right) = A_{lit}R_q^{hét} \quad (10)$$

Q species constituting waste is composed of MO (Organic Matter), Char, ash, and H_2O_liq. The reaction terms $R_q^{hét}$ are calculated based on the data in table 8.

As well as for the meal, mass conservation equation in the bed is modeled by the equation (11):

$$\frac{d}{dz}\left(A_{lit}u_{lit}y_{dec}^{lit}\rho_{lit}\right) = A_{lit}\sum_q R_q^{hét} \quad (11)$$

B1. Organic Matter

Dealing with the organic matter held in the incoming waste (and/or biomass) it has been chosen to follow its composition (in terms of ultimate analysis) all over the bed. Hence, equation (12) is derived where subscript "d" stands for atoms of C, H, O, N, S, and Cl. The mass conservation equation is modeled by the equation (12), where $R_d^{hét}$ is computed as a function of the heterogeneous rates of reactions and of the composition of the products of these reactions:

$$\frac{d}{dz}\left(\rho_{lit}A_{lit}u_{lit}y_d^{MO}y_{MO}^{dec}y_{dec}^{lit}\right) = A_{lit}R_d^{hét} \quad (12)$$

C. Gas

The equation (13) represents the mass conservation of b gas species (N_2, O_2, NO, CH_4, H_2, H_2O, CO, CO_2, H_2S, HCN, HCl, C_6H_6, $C_{10}H_8$, C_6H_6O, and C_7H_8).

$$\frac{d}{dz}\left(\rho_{lit}A_{lit}u_{lit}y_b^{gaz}y_{gaz}^{lit}\right) = A_{lit}\left(R_b^{homo} + R_{CO2}^{faV} + R_d^{decV}\right) \quad (13)$$

Where R_{CO2}^{faV} and R_d^{decV} represent respectively the formation rate of CO_2 produced by calcination reactions of meal, and the formation rate of gaseous species from the pyrolysis reaction and, gasification and combustion reactions of solid pyrolysis residue.

The mass conservation equation of gas in the bed is modeled by the equation (14).

$$\frac{d}{dz}\left(\rho_{lit}A_{lit}u_{lit}y_{gaz}^{lit}\right) = A_{lit}\left(\sum_d R_d^{decV} + R_{CO2}^{faV}\right) \quad (14)$$

Since neither mass cannot be created nor destroyed by homogeneous reaction in gas phase, the sum of homogeneous formation rate is zero ($\sum_b R_b^{homo} = 0$).

4.1.2.2. Bed Temperature

The enthalpy of the bed is computed by the equation (15) using the compositions of each species of the bed.

$$h_{lit}(z) = \left\{ \sum_{k=1}^{NCfaSol} y_k^{Sol}(z) \left(h_{f,k}^0 + \int_{T_{ref}}^{T_{lit}} c_{p,k}(T)dT \right) y_{fa}^{Sol} + \sum_{k=1}^{NCfaLiq} y_k^{Liq}(z)\left(h_{f,k}^0 + L_k\right) y_{fa}^{Liq} \right\} y_{fa}^{lit} + \left\{ \sum_{q=1}^{NCdec} y_q^{dec}(z) \left(h_{f,q}^0 + \int_{T_{ref}}^{T_{lit}} c_{p,q}(T)dT \right) \right\} y_{dec}^{lit} + \left\{ \sum_{b=1}^{NCgaz} y_b^{dec}(z) \left(h_{f,b}^0 + \int_{T_{ref}}^{T_{lit}} c_{p,b}(T)dT \right) \right\} y_{gaz}^{lit} \quad (15)$$

4.1.2.3. Energy conservation equation

The energy conservation equation in solid bed is modeled by equation (16) below:

$$\frac{d}{dz}(\rho_{lit} A_{lit} u_{lit} h_{lit}) = \varphi_{gazFB-L}^{Conv} l_{lit} + \varphi_{gazFB-L}^{Ray} l_{lit} + \varphi_{four-L}^{Cond} \pi d_1 + \varphi_{four-L}^{Ray} l_{lit} \quad (16)$$

The first member represents the energy variation in the solids bed. The second member represents the sum of the flows exchanged between the bed of solids (meal, and waste, and gas), the freeboard gas and the kiln wall. The various modes which the heat transfer in the bed occurs are given in figure 2 above. $\varphi_{gazFB-L}^{Conv}$, $\varphi_{gazFB-L}^{Ray}$,φ_{four-L}^{Cond} et φ_{four-L}^{Ray} are respectively the flow of specific heats exchanged by convection between the gas phase and the bed of material, by radiation between the gas phase and the bed of material, by conduction between the kiln walls and the bed, and by radiation between the kiln walls and bed. These are given in the table 9 below.

Exchange	Modes	Equations
Gas Freeboard-Bed	Convection	$\varphi_{gazFB-L}^{Conv} = h_{gazFB-L} A_{lit}^{l} (T_{gazFB} - T_{lit})$
	Radiation	$\varphi_{gazFB-L}^{Ray} = \sigma_B A_{lit}^{l} (\varepsilon_{lit} + 1) \left(\frac{\varepsilon_g T_{gazFB}^4 - \alpha_g T_{lit}^4}{2} \right)$
Gas freeboard-kiln	Convection	$\varphi_{gazFB-F}^{Conv} = h_{gazFB-F} A_{four}^{d} (T_{gazFB} - T_{four})$
	Radiation	$\varphi_{gazFB-F}^{Ray} = \sigma_B A_{four}^{d} (\varepsilon_{four} + 1) \left(\frac{\varepsilon_g T_{gazFB}^4 - \alpha_g T_{four}^4}{2} \right)$
Kiln-Bed	Conduction	$\varphi_{four-L}^{Cond} = h_{litF} A_{four}^{c} (T_{four} - T_{lit})$
	Radiation	$\varphi_{four-L}^{Ray} = \sigma_B . A_{lit}^{l} . \varepsilon_{lit} . \varepsilon_{four} . \Omega (T_{four}^4 - T_{lit}^4)$

Table 9: Heat exchange inside the rotary kiln [30]

Heat transfer coefficients for convection between gas freeboard and bed, and gas freeboard and kiln are calculated using relations given by Tsheng and Watkinson [31], returned by Mujumdar and al [30], and are given respectively by the equations (17) and (18) :

$$h_{gazFB-L} = 0.46 \frac{k_G}{D_e} Re_D^{0.535} Re_\omega^{0.104} \eta^{-0.341} \quad (17)$$

$$h_{gazFB-F} = 1.54 \frac{k_G}{D_e} Re_D^{0.575} Re_\omega^{-0.292} \quad (18)$$

4.1.2.4. Densities of bed

The bed density is modeled by the equation (19) below, where R_j represents the formation rates of gaseous species.

$$\frac{d}{dz}(\rho_{lit} A_{lit} u_{lit}) = -A_{lit} \left(R_{CO2}^{faV} + \sum_{j=1}^{NESGAZ} R_j \right) \quad (19)$$

4.1.2.5. Geometrical parameters of the kiln

A. Bed height

The evolution of the bed height is modeled by the equation (20) below, outcome of the work of Vahl and Kingma [32], of Kramers and al [33], and taken back by Mujumdar and al [30]. This model estimates the bed height at each position.

$$\frac{dH_{lit}(z)}{dz} = tg\ \varphi_{lit} \cdot \left[\frac{tg\ \delta_{four}}{sin\ \delta_{four}} - \frac{3q_v}{4\pi n_{four} r_1^3} \left(\frac{2H_{lit}(z)}{r_1} - \frac{{H_{lit}}^2(z)}{r_1^2} \right)^{-3/2} \right] \quad (20)$$

Where z is the axial position of the solids in rotary kiln, δ_{four} the inclination angle of kiln with the horizontal axis, q_v the volume flow, n_{four} the kiln rotational speed, and r_1 the radius of kiln.

B. Fill degree

The degree of filling, given by equation (21) below [34], is a very important factor to estimate the height of the bed at the inlet of rotary kiln.

$$f = \frac{1}{2\pi} \left(2\ cos^{-1} \left(\frac{r_1}{r_1 - H_{lit}(z=0)} \right) - sin \left[2\ cos^{-1} \left(\frac{r_1}{r_1 - H_{lit}(z=0)} \right) \right] \right) \quad (21)$$

A diagram is available in the literature which give the degree of filling based on the number Froude, rotational speed and height or depth of the bed. There exists acceptable ranges of the Froude number for each bed movement mode. The degree of filling is expressed as a percentage.

C. Repose angle of bed (kiln slope)

The repose angle of bed is an important geometrical factor in the axial motion of bed. It is also called the dynamic angle of repose, and is given by the equation (22) below. It is taken from the expression of average speed of axial transport (plug flow) along the rotary kiln [34].

$$cos\varphi_{lit}(z) = \frac{u_{lit}(z) sin\left(\frac{\delta_{lit}(z)}{2}\right) - 2\pi r_1 n_{four}\ \delta_{four}}{2\pi r_1 n_{four} \beta} \quad (22)$$

D. Intercept angle of bed

The intercept angle of bed is a fundamental greatness. It allows the determination of the width of the bed, the bed's repose angle, and other geometrical parameters of the kiln. It is given by the equation (23) below [27]:

$$\delta_{lit}(z) - sin(\delta_{lit}(z)) = \frac{8A_{lit}(z)}{d_1^2} \quad (23)$$

E. Transverse surface of bed

The transverse surface of bed is given by the equation (24) below [30] :

$$A_{lit} = \frac{1}{2} \left(r_1 \delta_{lit}(z) - l_{lit}(z).(r_1 - H_{lit}(z)) \right) \quad (24)$$

F. Width of bed (Mid Cord)

The width of the bed is also a significant magnitude in the study of the 1D model of the bed. It is given by the equation (25), derived from the geometry of the bed [1], [27].

$$l_{lit}(z) = d_1\ sin\left(\frac{\delta_{lit}(z)}{2}\right) \quad (25)$$

G. Angle between surface of bed material and kiln axis

Of the proceedings of Vahl and Kingma [32], we have explicited the angle between surface of bed material and kiln axis. In fact, since the bed height, from input to output is decreasing, it is necessary to estimate at each point in this angle, which is strongly linked to the bed height and angle at rest bed. It's given by the relation below (26):

$$\tan \beta\ (z) = -\frac{dH_{lit}}{dz} \quad (26)$$

5. CONCLUSIONS

A mathematical model for the thermochemical conversion of waste (Tires, RDF, and Biomass) in a cement rotary kiln production is presented. The model is devoted to the description of the thermochemical phenomena that occur when the waste is used as an alternative fuel in cement rotary kiln. Although the results are not yet available for the moment, has given insights on the development of 1D bed model. The main assumptions on which the model relies on have been proposed. Also, the main phenomena taken into account have been described (physicochemical reactions of meal and waste, heat transfer in the kiln, charge transport and evolution of bed height). Subsequently, a description of the system under study is given. It describes the various wastes considered in this work, from the kinetics and product of pyrolysis point of view. Finally, the mathematical equations of the model are provided. The expected results of the 1D model of bed will be coupled to a 3D model of CFD Fluent (freeboard) to describe the energy conversion processes occurring in a cement rotary kiln. This article is in fact a route to follow for the 1D modeling material bed when wastes are used as alternative fuels in cement rotary kilns.

REFERENCES

[1] J. D. Martínez, N. Puy, R. Murillo, T. García, M. V. Navarro, and A. M. Mastral, "Waste tyre pyrolysis – A review," *Renew. Sustain. Energy Rev.* **23**, 179–213 (2013).

[2] N. A. Madlool, R. Saidur, N. A. Rahim, M. R. Islam, and M. S. Hossian, "An exergy analysis for cement industries: An overview," *Renew. Sustain. Energy Rev.* **16**, 921–932 (2012).

[3] B.-J. R. Mungyeko Bisulandu and C. Pongo Pongo, "Les énergies renouvelables face à l'épuisement des énergies fossiles: Utilisation et Valorisation des déchets dans les fours de cimenterie.," in *7éme Édition COFRET* **COFRET'14/ 6/OF-025**, (Paris, France, 2014).

[4] U. Kääntee, R. Zevenhoven, R. Backman, and M. Hupa, "Cement manufacturing using alternative fuels and the advantages of process modelling," *Fuel Process. Technol.* **85**, 293–301 (2004).

[5] E. Mokrzycki, A. Uliasz-Bocheńczyk, and M. Sarna, "Use of alternative fuels in the Polish cement industry," *Appl. Energy* **74**, 101–111 (2003).

[6] K. T. Kaddatz, M. G. Rasul, and A. Rahman, "Alternative Fuels for use in Cement Kilns: Process Impact Modelling," *Procedia Eng.* **56**, 413–420 (2013).

[7] C. Di Blasi, "Dynamic behaviour of stratified downdraft gasifiers," in *Chem. Eng. Sci. 55 2000*.

[8] A. Aranda Usón, A. M. López-Sabirón, G. Ferreira, and E. Llera Sastresa, "Uses of alternative fuels and raw materials in the cement industry as sustainable waste management options," *Renew. Sustain. Energy Rev.* **23**, 242–260 (2013).

[9] (CINAT) Cimenterie Nationale, "Données techniques" (Service Controle Qualité, 2010).

[10] Ü. Çamdali, A. Erişen, and F. Çelen, "Energy and exergy analyses in a rotary burner with pre-calcinations in cement production," *Energy Convers. Manag.* **45**, 3017–3031 (2004).

[11] A. K. Chatterjee, "Chemistry and engineering of the clinkerization process — Incremental advances and lack of breakthroughs," *Cem. Concr. Res.* **41**, 624–641 (2011).

[12] A. A. Boateng and P.V. Barr, "A thermal model for the rotary kiln including heat transfer within the bed," 2131–2147 (1996).

[13] F. Marias, "A model of a rotary kiln incinerator including processes occurring within the solid and the gaseous phases," *Comput. Chem. Eng.* **27**, 813–825 (2003).

[14] P. DARABI, "A mathematical model for cement kilns" (University of British Columbia, 2007).

[15] Boris V. L'vov, "Mechanism and kinetics of thermal decomposition of carbonates," *Thermochim. Acta*, 1–16 (2002).

[16] R. Tartarelli and M. Seggiani, “Analisi e modellazione numerica del processo di gassificazione del carbone in reattori updraft” (Agenzia Nazionale per le Nuove Tecnologie, l’Energia e lo Sviluppo Economico Sostenibile, 2010).
[17] A. A. Boateng and P. V. Barr, “Modelling of particle mixing and segregation in the transverse plane of a rotary kiln,” *Chem. Eng. Sci.* **51**, 4167 4181 (1996).
[18] P. Bernada, F. Marias, A. Deydier, F. Couture, and A. Fourcault, “Modelling of a Traveling Bed WASTE Gasifier,” *Waste Biomass Valorization* **3**, 333–353 (2012).
[19] M. A. Gómez, J. Porteiro, D. Patiño, and J. L. Míguez, “CFD modelling of thermal conversion and packed bed compaction in biomass combustion,” *Fuel* **117**, 716–732 (2014).
[20] F. Marias, R. Demarthon, A. Bloas, and J. P. Robert-arnouil, “Modeling of tar thermal cracking in a plasma reactor,” *Fuel Process. Technol.* **149**, 139–152 (2016).
[21] P. T. Williams, “Pyrolysis of waste tyres: A review,” *Waste Manag.* **33**, 1714–1728 (2013).
[22] M. Materazzi, P. Lettieri, R. Taylor, and C. Chapman, “Performance analysis of RDF gasification in a two stage fluidized bed–plasma process,” *Waste Manag.* **47**, **Part B**, 256–266 (2016).
[23] J. Werther, M. Saenger, E.-U. Hartge, T. Ogada, and Z. Siagi, “Combustion of agricultural residues,” *Prog. Energy Combust. Sci.* **26**, 1–27 (2000).
[24] A. Rahman, M. G. Rasul, M. M. K. Khan, and S. Sharma, “Recent development on the uses of alternative fuels in cement manufacturing process,” *Fuel* **145**, 84–99 (2015).
[25] J. H. Chen, K. S. Chen, and L. Y. Tong, “On the pyrolysis kinetics of scrap automotive tires,” *J. Hazard. Mater.* **84**, 43–55 (2001).
[26] M. W. Seo, S. D. Kim, S. H. Lee, and J. G. Lee, “Pyrolysis characteristics of coal and RDF blends in non-isothermal and isothermal conditions,” *J. Anal. Appl. Pyrolysis* **88**, 160–167 (2010).
[27] F. Marias, H. Roustan, and A. Pichat, “Modelling of a rotary kiln for the pyrolysis of aluminium waste,” *Chem. Eng. Sci.* **60**, 4609–4622 (2005).
[28] E. Mastorakos, A. Massias, C.D. Tsakiroglou, D.A. Goussis, V.N. Burganos, and A.C. Payatakes, “CFD predictions for cement kilns including Flame modelling, heat transfer and clinker chemistry,” 55–76 (1999).
[29] K. S. Mujumdar and V. V. Ranade, “CFD modeling of rotary cement kilns,” *Asia-Pac. J. Chem. Eng.* **3**, 106–118 (2008).
[30] K. S. Mujumdar and V. V. Ranade, “Simulation of Rotary Cement Kilns Using a One-Dimensional Model,” *Chem. Eng. Res. Des.* **84**, 165–177 (2006).
[31] Tsheng S. H. and Watkinson A. P., “Convective heat transfer on rotary kilns,” in *Can J Chem Engg 57* (1979).
[32] L. Vàhl and W. G. Kingma, “Transport of solids through horizontal rotary cylinders,” *Chem. Eng. Sci.* **1**, 253–258 (1952).
[33] H. Kramers and P. Croockewit, “The passage of granular solids through inclined rotary kilns,” *Chem. Eng. Sci.* **1**, 259–265 (1952).
[34] A. A. Boateng, *Rotary kilns-Transport Phenomena and Transport Processes* (United States of America, 2012).